CHEMISTRY
A European Journal

A Journal of
ChemPubSoc Europe

Accepted Article

Title: Achieving photovoltaic devices showing high short circuit current approaching 15 mA cm-2 through a trihydroxyl substitution strategy on an unsymmetrical squaraine dye

Authors: Jianglin Wu, Changfeng Si, Yao Chen, Lin Yang, Bin Hu, Guo Chen, Zhiyun Lu, and Yan Huang

To be cited as: *Chem. Eur. J.* 10.1002/chem.201705140

Link to VoR: http://dx.doi.org/10.1002/chem.201705140

Supported by
ACES

WILEY-VCH

10.1002/chem.201705140

WILEY-VCH

Achieving photovoltaic devices showing high short circuit current approaching 15 mA cm^{-2} through a trihydroxyl substitution strategy on an unsymmetrical squaraine dye

Jianglin Wu, [a]§ Changfeng Si, [b]§ Yao Chen, [a] Lin yang, [a] Bin Hu, [a] Guo Chen,* [b] Zhiyun Lu, [a] and Yan Huang*[a]

Abstract: A series of unsymmetrical arene-1,3-squaraine-structured squaraine (USQ) derivatives bearing two, three or four hydroxyl (–OH) substituents, namely **USQ-2-OH**, **USQ-3-OH**, or **USQ-4-OH**, were designed and synthesized, and the effect of the hydroxyl number on the optoelectronic properties of USQs were investigated. Despite the three compounds show similar UV-Vis absorption and HOMO energy levels, solution-processed bulk-heterojunction small molecule organic solar cells (BHJ-SMOSCs) using **USQ-3-OH** as electron donor materials exhibits the highest power conversion efficiency (PCE) of 6.07%, which could be mainly attributed to the higher hole mobility and smaller phase separation. It is also noteworthy that the short circuit current (J_{sc}) of the USQ-3-OH–based device is as high as 14.95 mA cm^{-2}, which is, to the best of our knowledge, the highest J_{sc} data for the squaraine-based BHJ solar cell up to now. Our results also indicated that more –OH substituents on squaraine dyes will not necessarily leads to better photovoltaic performance.

Introduction

Owing to their attractive advantages of low cost, low weight, and potential of fabricating flexible devices by roll-to-roll technique, organic solar cells (OSCs) are considered as one of the most promising green energy alternatives for future renewable energy conversion.[1] Among the multifarious kinds of electron donor materials, squaraine (SQ) dyes have drawn much recent attention due to their intense and broad absorption in the Vis-NIR spectral regions and excellent photochemical and photophysical stability.[2] Thanks to the endeavored efforts of the researchers, many high-performance organic photovoltaic (OPV) SQ dyes have been acquired successfully. In most cases, high-performance OPV SQ derivatives should possess hydroxyl (–OH) substituents which can be capable of forming intramolecular hydrogen bonds (HBs) with the squaric ring. [2f, 3] However, only two reports investigated the effect of hydroxyl on photovoltaic performance.[4] Kido et al found that for DBSQ (shown in Figure 1) and its analogs bearing decreasing even number of hydroxyl substituents (two or zero), their OPV performance dropped

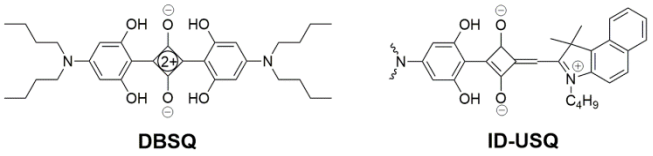

Figure 1. Structure of DBSQ and ID- USQ

monotonously;[4a] our recent research discoveries indicated that for unsymmetrical squaraine (USQ, D-A-D'-structured) derivatives bearing 1,1,2-trimethyl-1*H*-benzo[*e*]indole as the D and hydroxy-substituted phenyl derivatives as the D' subunits (ID-USQ, shown in Figure 1), the presence of 2,6-dihydroxy in these compounds triggered better OPV performance with power conversion efficiency (PCE) of >5%.[3e, 3f]

Based on these previous findings, it seems reasonable to infer that the presence of more –OH groups capable of forming intramolecular hydrogen bonds (HBs) might endow SQ derivatives with more improved photovoltaic performance. However, no systematic research works have been carried on SQ dyes bearing all kinds of possible hydroxyl substituents, it should be cautious to draw a conclusion that "the larger number of hydroxyl substituents in SQ derivatives, the better OPV performance"

Nonetheless, for arene-1,3-squaraine-typed symmetrical squaraine (SSQ) derivatives like DBSQ, it is impossible to construct compounds bearing odd –OH groups. while for arylidene-1,3-squaraine-typed USQs, their available number of –OH groups will be less than two. Hence if we could exploit arene-1,3-squaraine-structured USQ derivatives, they may show compromised odd number and larger number of –OH groups.

However, to the best of our knowledge, so far no such photovoltaic USQ derivatives bearing an unsymmetrical arene-1,3-squaraine structure bearing three OH groups could be found. Consequently, in this contribution, we designed and synthesized a series of novel arene-1,3-squaraine-structured USQ compounds bearing not only even number (two or four), but also odd number (three) of hydroxyl substituents (**USQ-2-OH**, **USQ-3-OH**, and **USQ-4-OH**, as illustrated in Figure 2). In comparison with SSQ derivatives, the resultant objective USQ compounds could not only possess odd –OH groups, but also display better structural diversity hence fine-tuned optoelectronic properties and better solubility; while compared to arylidene-1,3-squaraine-typed USQ, these objective compounds could possess more –OH substituents. In-depth structure-property relationship studies revealed that the number of –OH substituents has negligible influence on the UV-Vis absorption properties of these compounds; with increasing number of –OH substituents, the highest occupied molecular orbital (HOMO) level of the compound will decline slightly; interestingly, the trihydroxyl substituted compound **USQ-3-OH** displays the

[a] Jianglin Wu, Yao Chen, Lin yang, Bin Hu, Zhiyun Lu, Dr. Yan Huang
Key Laboratory of Green Chemistry and Technology (Ministry of Education), College of Chemistry, Sichuan University, Chengdu 610064, P. R. China.
E-mail: huangyan@scu.edu.cn
[b] Changfeng Si, Dr. Guo Chen
Key Laboratory of Advanced Display and System Applications, Ministry of Education, Shanghai University, 149 Yanchang Road, Shanghai, 200072, P. R. China.
[§] These authors contributed equally.

Supporting information for this article is given via a link at the end of the document.

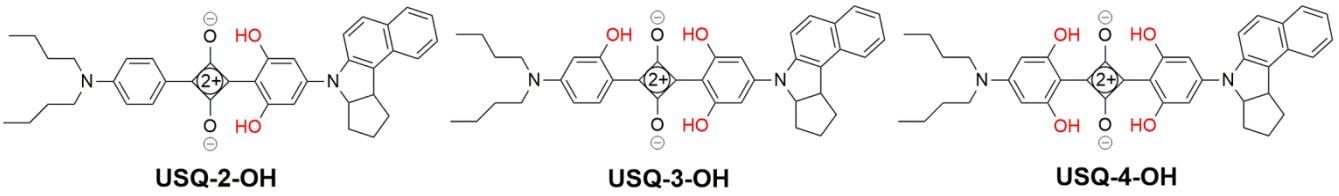

Figure 2. Structure of USQ-2-OH, USQ-3-OH and USQ-4-OH

highest photovoltaic performance among all these three compounds, which should arise from the higher hole mobility and smaller phase separation of the **USQ-3-OH** : $PC_{71}BM$ blending photoactive film. It is noteworthy that the short circuit current (J_{sc}) of **USQ-3-OH**-based device could be as high as 14.95 mA·cm^{-2}, which is the highest value among SQ-based BHJ solar cells; and the PCE of **USQ-3-OH**-based device could reach 6.07%, which is also one of the highest PCE data among SQ-based BHJ solar cells. [3f, 3h, 5]

Results and Discussion

Synthesis and characterization

Compound **USQ-2-OH** was synthesized *via* two-step condensation reactions between squaryl chloride and reactant **2a** (resulting in intermediate **3a,** and getting **4a** undergo hydrolysis), then intermediate **4a** and **5**, as described in our previous report.[3g] Similarly, **USQ-3-OH** could be prepared with high yield of 95% in the last step. However, in the case of **USQ-4-OH**, it could not be obtained *via* this two-step concentration procedure, since the intermediate **3c** could not be prepared successfully under the similar reaction conditions due to the rather high reactivity of the reactant **2c**. Nevertheless as according to literature reports, symmetric SQ dyes could be synthesized through one-pot two-step condensation reactions between squaric acid and electron-rich reactant,[6] we tried to use both **5** and **2c** as the electron-rich species to concentrate with squaric acid, and finally obtained not only the symmetrical by-products, but also the unsymmetrical objective compound **USQ-4-OH** successfully. The molecular structures of all these objective compounds were confirmed by ^{1}H NMR, ^{13}C NMR, FT-IR and HR-MS. As shown in Figure 3a, the chemical shifts of the hydroxyl protons of all these objective compounds are all observed to be significantly downfield-shifted into 10.8-13.0 ppm, indicative of the presence of relatively strong intramolecular HBs between the –OH substituent and the carbonyl group of the squaric ring in these compounds.[7] However, with increasing hydroxyl substituent number, the proton signals of the –OH groups of these USQ compounds are upfield-shifted gradually: δ = 12.84 ppm for **USQ-2-OH**; δ = 12.04, 11.32, and 10.95 ppm for **USQ-3OH**; δ = 11.10; 10.82 ppm for **USQ-4-OH**, suggesting

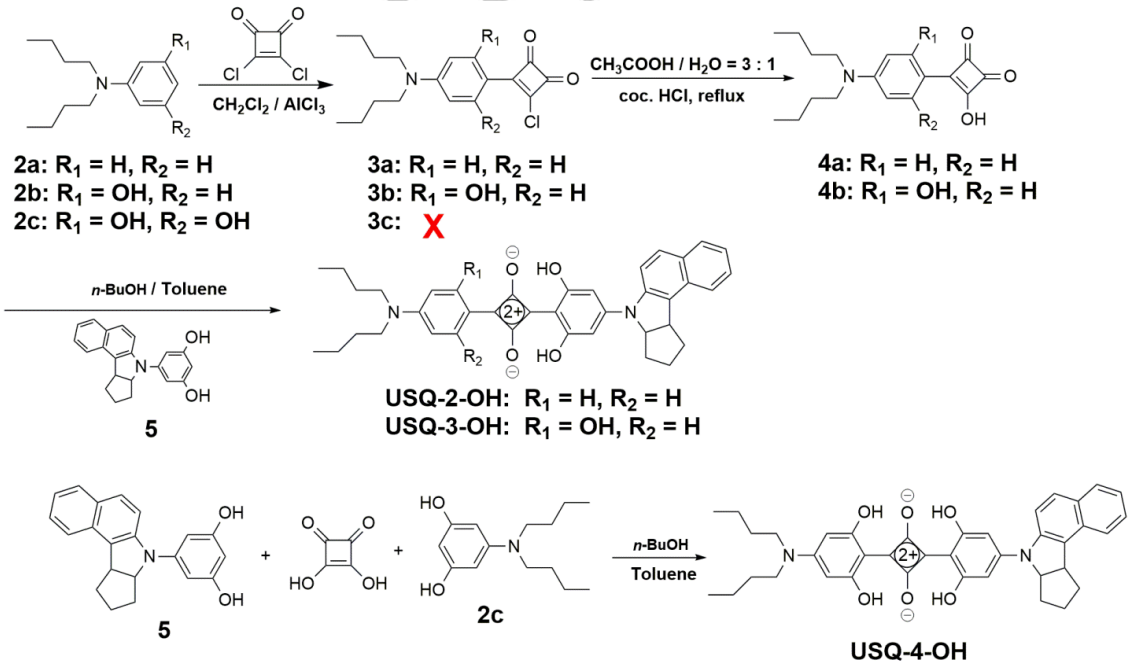

Scheme 1. Synthetic Routes to the objective compounds

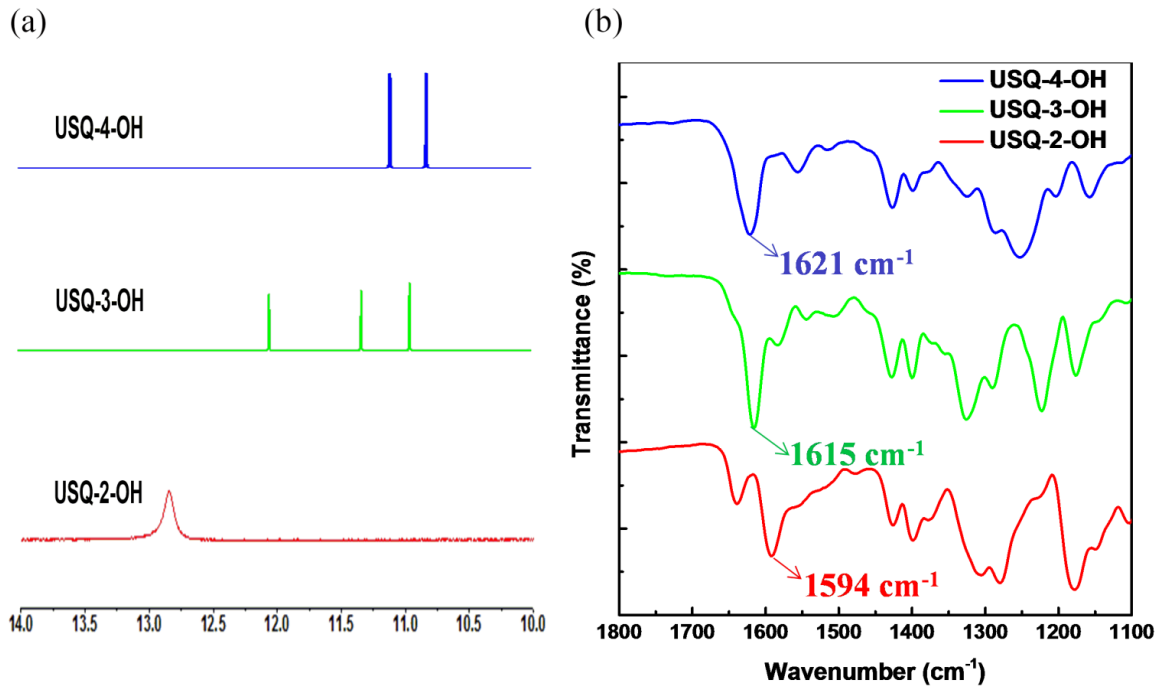

Figure 3. (a) FT-IR spectra of the objective compounds and (b) ^{1}H NMR spectra of corresponding to the proton signals of the –OH groups.

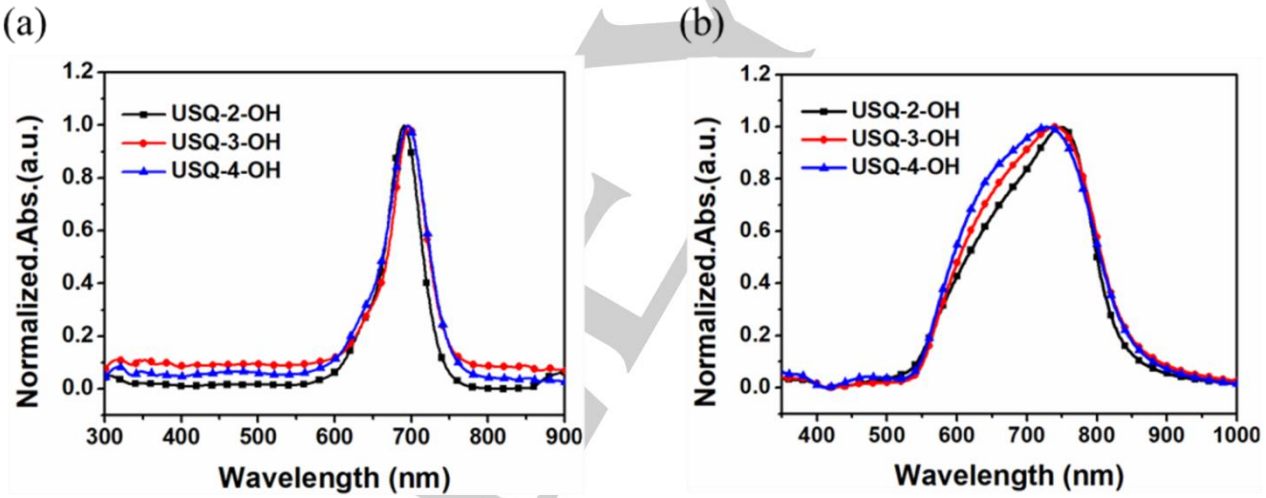

Figure 4. Absorption spectra of the objective compounds in (a) solution; and (b) thin film states.

that the presence of more –OH substituents trigger weakened intramolecular HB interactions. This deduction is further confirmed by FT-IR characterization results on these USQ compounds. As shown in Figure 3b, the characteristic stretching vibration signals of the carbonyl functional group of their resonance-stabilized zwitterionic 1,3-squaraine unit[8] are found to be blue-shifted with increasing –OH substituent number (1594 cm^{-1} for **USQ-2-OH**; 1615 cm^{-1} for **USQ-3-OH**; and 1621 cm^{-1} for **USQ-4-OH**), indicative of the gradually weakened intramolecular HB interactions in these compounds.[9] It is noteworthy that the difference in wave number is 21 cm^{-1} between **USQ-2-OH** and **USQ-3-OH**, but only 6 cm^{-1} between **USQ-3-OH** and **USQ-4-OH**, implying that although the introduction of an additional –OH substituent in **USQ-2-OH** can induce obvious variation on the HB strength, the grafting of an extra –OH substituent at **USQ-3-OH** only trigger less significant influence on the HB strength.

Optical and Electrochemical Characterization

The optical properties of three USQ dyes were investigated via UV-Vis absorption spectra in both dilute chloroform solution (2 × 10^{-6} M) and thin film states (data summarized in Table 1). As depicted in Figure 4a and 4b, in both solution and thin solid film states, these three USQ dyes display analogous absorption

Table 1 Optical and Electrochemical Properties of the Objective Compounds

Compd.	λ_{abs} (nm) [a] (log ε)	λ_{abs} [b] (nm)	FWHM (nm) Solution	FWHM (nm) Film	E_g^{opt} [c] (eV)	E_{ox} [d] (V)	HOMO [e] (eV)	LUMO [f] (eV)
USQ-2-OH	691(5.24)	748	53	184	1.47	0.32	–5.12	–3.65
USQ-3-OH	696(5.03)	740	56	206	1.45	0.33	–5.13	–3.68
USQ-4-OH	695(5.14)	730	63	212	1.44	0.36	–5.16	–3.72

[a] Measured in 2.0×10^{-6} mol L^{-1} $CHCl_3$ solution. [b] Thin films casted from 5 mg mL^{-1} $CHCl_3$ solution on quartz substrates. [c] Obtained from the onset of UV-Vis absorption spectra in thin film state. [d] Oxidation potential values were measured by cyclic voltammetry vs. Fc/Fc^+. [e] HOMO energy levels were deduced from the equation of HOMO = – (E_{ox} + 4.80) eV. [f] LUMO energy levels were deduced from the equation LUMO = HOMO + E_g^{opt}

characters. However, consistent with the FT-IR characterization results, in dilute solution, the absorption spectrum of **USQ-2-OH** (λ_{abs} = 691 nm) is slightly blue-shifted than that of **USQ-3-OH** (λ_{abs} = 696 nm) or **USQ-4-OH** (λ_{abs} = 695 nm), but the absorption spectra of USQ-3-OH and USQ-4-OH nearly resemble each other. In thin films, all these three USQ dyes display red-shifted and drastically broadened absorption bands than their corresponding solution samples, which could be attributed to the aggregation of USQ molecules.[10] From the onset absorption wavelengths of their film samples, the optical gaps of **USQ-2-OH**, **USQ-3-OH** and **USQ-4-OH** were estimated to be 1.47, 1.45 and 1.44 eV, respectively, all are close to the optimum bandgap (1.1~1.5 eV) for photovoltaic electron donor applications in constructing single-junction cell.[11]

The energy levels of the frontier molecular orbitals of the objective compounds were evaluated by cyclic voltammetry (CV) in CH_2Cl_2 solution (cyclic voltammograms were depicted in Figure S2, relevant data were summarized in Table 1). By comparison their oxidation potentials with Fc/Fc^+ redox couple, the HOMO energy levels were calculated to be –5.12, –5.13 and –5.16 eV for **USQ-2-OH**, **USQ-3-OH** and **USQ-4-OH**, respectively; while the LUMO energy level of these USQ dyes were calculated to be –3.65 eV for **USQ-2-OH**, –3.68 eV for **USQ-3-OH**, and –3.72 eV for **USQ-4-OH** through their HOMO level and corresponding optical bandgap data. By comparing the HOMO energy level data of these compounds, it could be inferred that the increasing number of –OH substituents in these USQ derivatives induce gradually declined HOMO energy level. This observation is consistent with that of Kido and coworker, which should be attributed to the reduction of the overall energy in the SQ fluorophore due to the intramolecular HB-induced extension of the conjugated structures.[4a] For all these three USQ compounds, their LUMO levels are more than 0.3 eV higher than that of $PC_{71}BM$, which could promote efficient exciton dissociation and charge separation in the blending system of $PC_{71}BM$/USQ.[12]

Photovoltaic characteristics

In order to investigate the effect of the number of –OH substituents on the photovoltaic performance of these USQs, BHJ-OPV cells with them as electron donor materials and [6,6]-phenyl-C_{71}butyric acid methyl ester ($PC_{71}BM$) as electron acceptor material were fabricated with device structure of ITO/MoO_3 (6 nm) /USQ:$PC_{71}BM$ (70 ± 5 nm) /Liq (1 nm) /Al (100 nm), and the USQ:$PC_{71}BM$ blending ratio was 1:3 or 1:5 in wt%. As depicted in Table 2, although 1:3 is a more optimum doping ratio than 1:5, in both cases, the **USQ-2-OH**-based devices are found to exhibit the worst photovoltaic performance with respect to PCE among all these three devices. This observation is in accordance with the previous reports that SQ derivatives bearing less –OH substituents would display poorer OPV performance.[4] Nevertheless, it is a little surprising that the photovoltaic performance of **USQ-4-OH** is inferior to that of **USQ-3-OH** (PCE: 6.07% vs. 5.67%) despite the fact that **USQ-4-OH** possesses more –OH substituents than **USQ-3-OH**. In fact the PCE value of 6.07%, to the best of our knowledge, is one of the highest PCE data among the reported squaraine based BHJ-OPV cells.[3f, 3h, 5]

To gain insight to the reason accounting for the higher photovoltaic performance of **USQ-3-OH** than **USQ-2-OH** and **USQ-4-OH**, comparison studies were carried on the open circuit voltage (V_{oc}), J_{sc} and fill factor (FF) of these 1:3 USQ:$PC_{71}BM$-based devices. As depicted in Figure 5a and Table 2, the FF of the three devices are quite analogous; the V_{oc} of the **USQ-4-OH** based device (0.86 V) is slightly higher than that of the **USQ-3-OH-** (0.82 V) or **USQ-2-OH**-based device (0.82 V), which should be attributed to the more declined HOMO energy level of **USQ-4-OH** than **USQ-2-OH** and **USQ-3-OH**; but as far as J_{sc} is concerned, the **USQ-3-OH**-based device shows much higher J_{sc} (14.95 mA cm^{-2}) than that of **USQ-2-OH** (13.05 mA cm^{-2}) or **USQ-4-OH** (12.58 mA cm^{-2}). Note that the J_{sc} value of 14.95 mA cm^{-2} is among the highest one in the reported squaraine based BHJ-OPV cells.

In general, J_{sc} correlates highly with the light harvesting capability, carrier mobility, and morphology characteristics of the active layer.[13] To elucidate the origin of the enhanced J_{sc} in **USQ-3-OH**-device, the EQE curves of the three devices were measured. As shown in Figure 5b, in the region of 350-850 nm, the **USQ-3-OH**-device shows higher EQE values than the other two devices. Taking into consideration that **USQ-3-OH** displays quite similar absorption characters with **USQ-4-OH** in thin film state, and only slightly broadened absorption than **USQ-2-OH** in 550-750 nm (Figure 4b), the increased J_{sc} in **USQ-3-OH**-device should be attributed to the different charge transport and film morphological properties of the active layer. To verify this hypothesis, the hole mobility of the active layers were determined via space charge limited current (SCLC) method, and the film morphological properties of the active layer were investigated through atomic force microscopies (AFM) and transmission electron microscopy (TEM) characterizations. As summarized in Figure S3 and Table 2, the hole mobility of the USQ:$PC_{71}BM$ active layers were calculated to be 4.34×10^{-5}, 1.16×10^{-4}, and 8.05×10^{-5} cm^2 V^{-1} s^{-1} for **USQ-2-OH**-, **USQ-3-OH**- and **USQ-4-OH**-based layers, respectively. Obviously, the **USQ-3-OH**-based active layer shows higher hole-mobility than both **USQ-4-OH**- and **USQ-2-OH**-based ones. In addition, although according to AFM characterizations on these active layers, all the three USQ:$PC_{71}BM$ (1:3) blending films exhibit similar uniform surface morphology with rather small root-mean-square (RMS) of 0.23-0.37 nm (Figure S4), further TEM characterization results indicated that the **USQ-3-OH**:$PC_{71}BM$

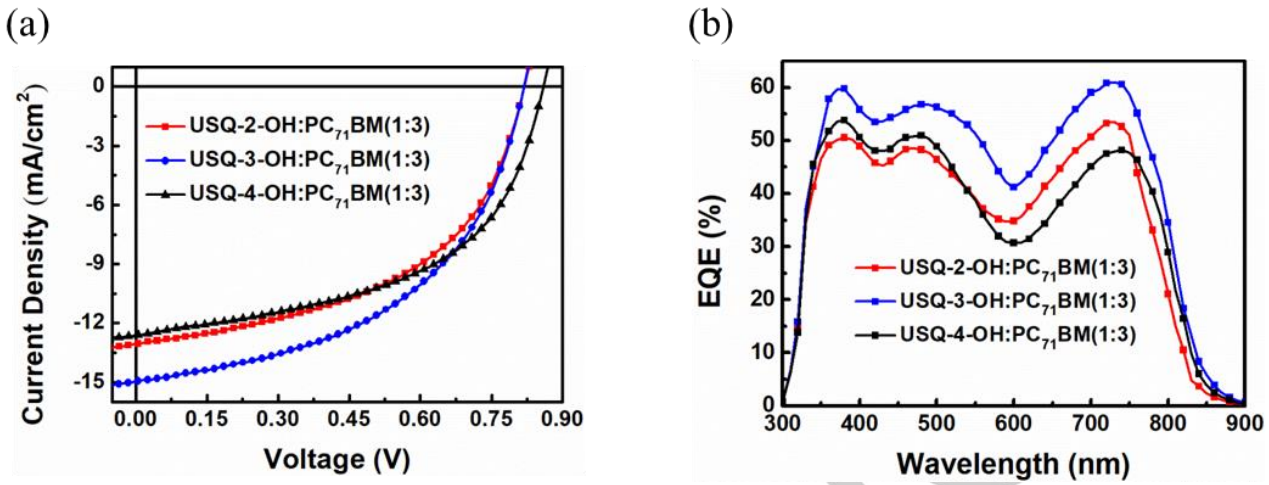

Figure 5. (a) *J*–V characteristics of the three USQ:$PC_{71}BM$ (1:3) devices (under AM 1.5 G solar spectrum at 100 mW cm^{-2} illumination); (b) EQE spectra of the three

Table 2. Photovoltaic Performances of OSCs with USQs:$PC_{71}BM$ as the Active Layer

Active layer (w/w)	J_{sc} (mA/cm^2)	V_{oc} (V)	FF (%)	PCE (%)[b]	μ_h(cm^2 V^{-1} s^{-1})
USQ-2-OH:$PC_{71}BM$ (1:3)[a]	13.05 (12.73)	0.82 (0.82)	51 (51)	5.40 (5.28)	4.34×10^{-5}
USQ-3-OH:$PC_{71}BM$ (1:3)[a]	14.95 (14.63)	0.82 (0.82)	50 (50)	6.07 (5.96)	1.16×10^{-4}
USQ-4-OH:$PC_{71}BM$ (1:3)[a]	12.58 (12.44)	0.86 (0.86)	52 (51)	5.67 (5.59)	8.05×10^{-5}
USQ-3-OH:$PC_{71}BM$ (1:5)[a]	14.13 (13.89)	0.83 (0.82)	50 (50)	5.79 (5.70)	9.13×10^{-5}
USQ-4-OH:$PC_{71}BM$ (1:5)[a]	13.05 (12.86)	0.88 (0.87)	48 (48)	5.47 (5.43)	6.65×10^{-5}
USQ-2-OH:$PC_{71}BM$ (1:3)[a, c]	13.13	0.83	49	5.34 (5.24)	
USQ-2-OH:$PC_{71}BM$ (1:3)[c]	12.87	0.84	46	4.97 (4.92)	
USQ-2-OH:$PC_{71}BM$ (1:5)[c]	10.97	0.85	49	4.57 (4.46)	

[a] Thermally annealed at 70 ºC for 10 min.[b] Average values of 12 individual cells were given in parentheses.[c] Reference from our previous reported studies

composition film shows the smallest phase separation size among all the three samples (Figure 6), which could promote more efficient charge separation at the D/A interface hence higher J_{sc}.[13] Consequently, the much higher J_{sc} of **USQ-3-OH**-based device than **USQ-2-OH**- and **USQ-4-OH**-based devices should be attributed to the higher hole mobility and smaller phase separation size of the corresponding photovoltaic active layer.

Conclusions

In summary, to unveil the correlations between the number of –OH substituents capable of forming intramolecular hydrogen bond and the photovoltaic properties of squaraine derivatives, we designed and synthesized a series of arene-1,3-squaraine-structured unsymmetrical rather than symmetrical squaraine derivatives bearing two, three or four hydroxy substituents. The results indicated that the number of –OH substituents has negligible influence on the UV-Vis absorption properties of these compounds, but the presence of more hydroxy groups could trigger more declined HOMO level of these compounds. In contrast to the current findings that "larger number of hydroxy substituents in SQ derivatives may trigger better OPV performance", we found that among all these three objective compounds, it is not the tetrahydroxy substituted **USQ-4-OH**, but the trihydroxy substituted **USQ-3-OH** that show the best photovoltaic performance. Note that both the PCE of 6.07% and J_{sc} of 14.95 mA·cm^{-2} of the **USQ-3-OH**-based device fall in the highest data of squaraine-based BHJ solar cells, and the high performance of the **USQ-3-OH**-device stems from the higher hole mobility and smaller phase separation of its photoactive layer. Taking advantages of their compromised better structural diversity, better solubility and probability for owning odd –OH substituents, arene-1,3-squaraine-structured unsymmetrical squaraines should be more promising candidates as

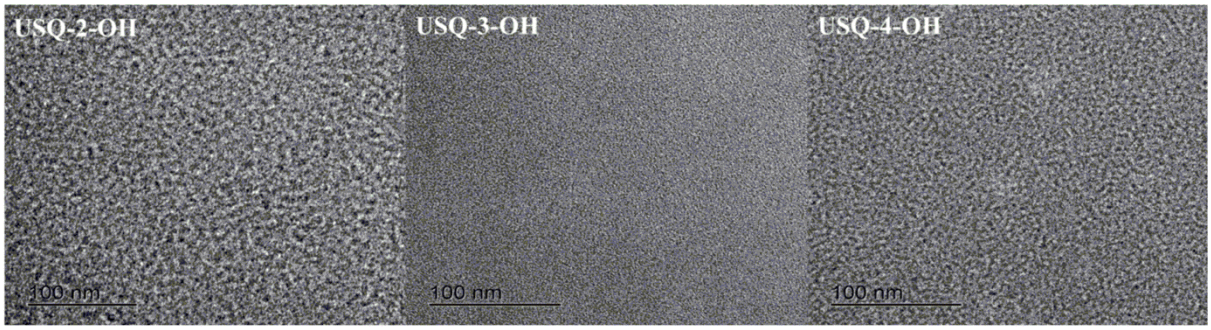

Figure 6. TEM images of the USQ:$PC_{71}BM$ (1:3) active layers

photovoltaic electron donor materials than their symmetrical counterparts.

Experimental Section

Instruments and Characterization

^1H NMR and ^{13}C NMR spectra were recorded on a Bruker Avance AVII (400 MHz) instrument with tetramethylsilane as the internal standard. High resolution mass spectra were measured on a Waters Q-TOF Premier. Absorption spectra of the target compounds in 2 × 10^{-6} M chloroform solution and thin film states were measured with a Perkin-Elmer Lambda 950 UV-Vis scanning spectrophotometer. Fourier transform infrared (FT-IR) spectra were recorded on a Perkin-Elmer 2000 infrared spectrometer with KBr pellets under ambient atmosphere. The morphologies of the blend films were analyzed through atomic force microscopy (AFM) in tapping mode under ambient conditions (MFP 3D Asylum Research instrument), and transmission electron microscopy (TEM) investigation was performed on Philips Technical G2 F20 at 200 kV. Cyclic voltammetry (CV) experiments were performed on a LK2010 Electrochemical workstation with a scan rate of 100 mV s^{-1}. All CV measurements were carried out at room temperature with a conventional three-electrode configuration employing a Pt disk as the working electrode, a Pt wire as the counter electrode, and a $Ag/AgNO_3$ as the reference electrode. Dichloromethane was freshly distilled from Phosphorus pentoxide (P_2O_5) under dry nitrogen. Tetrabutylammonium perchlorate (0.1 M) and ferrocenium/ferrocene redox couple (with an absolute energy of –4.80 eV *vs*. vacuum) were used as the supporting electrolyte and internal potential reference, respectively. The HOMO energy levels of these USQ dyes were calculated from the peak of the first oxidation waves by comparison with the Fc/Fc^+ redox couple according to the equation of HOMO = – (E_{ox} + 4.80) (eV); while the corresponding lowest unoccupied molecular orbital (LUMO) energy level of these USQ dyes were calculated through their HOMO level and optical bandgap data according to the equation of LUMO = HOMO + E_g (eV). The samples for atomic force microscopy (AFM) measurements were prepared by spin-casting the blending solution of USQ/$PC_{71}BM$ (1:3 in wt%) on glass substrates. Samples for TEM measurement were prepared by spin-casting the blending solution of USQ/$PC_{71}BM$ (1:3 in wt%) on PEDOT:PSS-coated ITO substrates, then floating the films on a water surface and transferring them to the TEM grids.

Synthesis

The synthetic routes of intermediates are shown in Scheme S1 and target molecules are outlined in scheme 1. Compounds **4a**, **4b**, **2c and 5** were prepared according to the procedures described in the literature.[2a[2a, 3g, 7a, 14] Dichloromethane, *n*-butanol and toluene were freshly distilled from P_2O_5, magnesium and sodium, respectively.

4-(4-(Dibutyliminio)-2-hydroxycyclohexa-2,5-dien-1-ylidene)-2-(2,6-dihydroxy-4-(8,9,10,10a-tetrahydrobenzo[*e*]cyclopenta[*b*]indol-7(7a*H*)-yl)phenyl)-3-oxocyclobut-1-enolate [**USQ-3-OH**]. A mixture of compounds **4b** (0.42 g, 1.33 mmol) and **5** (0.42 g, 1.33 mmol) in *n*-butanol (20 mL) and toluene (20 mL) was refluxed at 120 °C under Ar for 10 h, then the reaction mixture was cooled down. After removal of the solvent, the resultant crude product was purified by column chromatography (dichloromethane) followed by recrystallization from dichloromethane/*n*-hexane to give **USQ-3-OH** as a golden yellow solid (0.77 g, 95%). ^1H NMR (400 MHz, $CDCl_3$, ppm) δ: 12.04 (s, 1H, -OH), 11.32 (s, 1H, -OH), 10.95 (s, 1H, -OH), 7.88 (d, *J* = 9.6 Hz, 1H, ArH), 7.81 (d, *J* = 8.0 Hz, 1H, ArH), 7.76 (d, *J* = 8.4 Hz, 1H, ArH), 7.72(d, *J* = 8.0 Hz, 1H, ArH),7.65 (d, *J* = 9.2 Hz, 1H, ArH), 7.46 (t, *J* = 8.0 Hz, 1H, ArH), 7.34 (t, *J* = 8.0 Hz, 1H, ArH), 6.39-6.37 (m, 2H, ArH), 6.34 (dd, J_1 = 9.2 Hz, J_2 = 2.4 Hz, 1H, ArH), 6.11 (d, *J* = 2.4 Hz, 1H, ArH), 4.92-4.87 (m, 1H, CH), 4.32-4.27 (m, 1H, CH), 3.39 (t, *J* = 7.6 Hz, 4H, CH_2), 2.34-2.17 (m, 2H, CH_2), 2.08-1.97 (m, 2H, CH_2), 1.74-1.60 (m, 5H, CH_2), 1.54-1.48 (m, 1H, CH_2), 1.43-1.34 (m, 4H, CH_2), 0.99 (t, *J* = 7.2 Hz, 6H, CH_3). ^{13}C NMR (100 MHz, $CDCl_3$, ppm) δ: 181.3, 168.9, 165.7, 163.5, 162.9, 156.7, 153.7, 140.6, 132.7, 130.2, 128.8, 128.6, 124.2, 123.2, 114.9, 109.2, 108.1, 105.7, 98.6, 97.2, 69.6, 51.5, 44.7, 35.1, 33.5, 29.8, 24.9, 20.2, 13.9. FT-IR: *ν* ν = 1616 cm^{-1}. HRMS (ESI-TOF) m/z: $[M + H]^+$ Calcd. for $C_{39}H_{41}O_5N_2$, 617.3010; found, 617.3069.

4-(4-(Dibutyliminio)-2,6-dihydroxycyclohexa-2,5-dien-1-ylidene)-2-(2,6-dihydroxy-4-(8,9,10,10*a*-tetrahydrobenzo[*e*]cyclopenta[*b*]indol-7(7a*H*)-yl)phenyl)-3-oxocyclobut-1-enolate [**USQ-4-OH**]. A mixture of compound 2c (0.79 g, 1.96 mmol), 5 (1.13 g, 3.55 mmol) and squaric acid (0.34 g, 2.96 mmol) were dissolved in 20 mL toluene and 20 mL *n*-butanol, and refluxed at 120 °C under Ar for 10 h. Then the reaction mixture was cooled down, and the solvents were removed in vacuum. The resultant crude product was purified by column chromatography (eluent: dichloromethane) followed by recrystallization from dichloromethane/n-hexane to yield **USQ-4-OH** as a green solid (110 mg, 8.8%) as well as by product (DBSQ) with yield of 14.4%, characterization in Supporting Information. ^1H NMR (400 MHz, $CDCl_3$, ppm) *δ*: 11.10 (s, 2H, -OH), 10.82 (s, 2H, -OH), 7.79 (d, *J* = 8.0 Hz, 1H, ArH), 7.73 (d, *J* = 8.4 Hz, 1H, ArH), 7.70 (d, *J* = 8.8 Hz, 1H, ArH), 7.60 (d, *J* = 8.8 Hz, 1H, ArH), 7.41 (t, *J* = 8.0 Hz, ArH), 7.29 (d, *J* = 7.6 Hz, 1H, ArH), 6.35 (s, 2H, ArH), 5.75 (s, 2H, ArH), 4.93-4.88 (m, 1H, CH), 4.30-4.25 (m, 1H, CH), 3.73 (t, *J* = 7.6 Hz, 4H, CH_2), 2.33-2.23 (m, 1H, CH_2), 2.22-2.13 (m, 1H, CH_2), 2.07-1.95 (m, 2H, CH_2), 1.71-1.59 (m, 5H, CH_2), 1.54-1.44 (m, 1H, CH_2), 1.42-1.32 (m, 4H, CH_2), 0.98 (t, *J* = 7.6 Hz, 6H, CH_3). ^{13}C NMR (100 MHz, $CDCl_3$, ppm) δ: 163.2, 162.9, 162.0, 159.5, 158.8, 152.5, 140.8, 130.4, 130.2, 129.8, 128.7, 128.5, 126.7, 124.0, 123.0, 114.7, 104.2, 103.6, 97.6, 93.9, 69.5, 51.6, 44.6, 35.0, 33.6, 30.1, 24.9, 20.2, 13.8. FT-IR: ν = 1622 cm^{-1}.

HRMS (ESI-TOF) m/z : $[M + H]^+$ Calcd. for $C_{39}H_{41}O_6N_2$, 633.2959; found, 633.2971.

Device fabrication

The BHJ cells bearing USQ:$PC_{71}BM$ photoactive layer were fabricated as follow: patterned indium-tin-oxide (ITO) coated glass substrates were cleaned using detergent, deionized water, acetone and isopropanol in sequence in an ultrasonic bath. Cleaned substrates were dried and kept in an oven at 80 °C and exposed to UV ozone for 30 min, and then were immediately transferred into a high-vacuum chamber (1×10^{-5} Pa) for the deposition of 6 nm MoO_3 thin layer. Photoactive layers with thickness of 70 ± 5 nm were fabricated by spin-coating USQ:$PC_{71}BM$ solution (20 mg mL^{-1} in chloroform) on the MoO_3 pre-coated ITO substrates in a N_2-filling glove box, followed by additional thermal treatment at 70 ºC for 10 min. Finally, the substrates were transferred back to a high-vacuum chamber where 8-hydroxyquinolatolithium (Liq, 1 nm) and Al (100 nm) were deposited as the top electrode. Liq and MoO_3 were used as the n- and p-type interfacial layers, respectively. The active area of each cell is 0.04 cm^2 defined by the overlap of the ITO anode and the Al cathode. The final device structure was ITO/MoO_3 (6 nm) /USQ:$PC_{71}BM$ (70 ± 5 nm) /Liq (1 nm) /Al (100 nm). To obtain the average data related to device performance, two batches of devices (6 cells per batch) for each set of conditions were fabricated and tested. In addition, the SCLC (space-charge-limited-current) model was employed to characterize the carrier mobilities in the blend films, and hole-only devices were fabricated with a structure of ITO/MoO_3 (6 nm) /USQ:$PC_{71}BM$ (70 nm, 1:3 in wt%) /MoO_3 (6 nm) /Al.

Acknowledgements

We acknowledge the financial support for this work from the National Natural Science Foundation of China (project No.51573108, 61604093, 21372168), the Natural Science Foundation of Shanghai (16ZR1411000) and the Shanghai Pujiang Program (16PJ1403300). We also would like to thank Dr. Peng Wu of Analytical & Testing Center, Sichuan University, for his help in photophysical measurements.

Keywords: Unsymmetrical squaraine (USQ) 1 • hydroxyl substituent 2 • hole mobility 3 • bulk heterojunction (BHJ) photovoltaic cells 4

[1] a) H. Yao, L. Ye, H. Zhang, S. Li, S. Zhang, J. Hou, *Chemical reviews* 2016, *116*, 7397-7457; b) P. Cheng, X. Zhan, *Chem Soc Rev* 2016, *45*, 2544-2582; c) R. F. Service, *Science* 2011, *332*, 293-293.

[2] a) Y. Chen, Y. Zhu, D. Yang, Q. Luo, L. Yang, Y. Huang, S. Zhao, Z. Lu, *Chemical communications* 2015, *51*, 6133-6136; b) S. Karak, P. J. Homnick, A. M. Della Pelle, Y. Bae, V. V. Duzhko, F. Liu, T. P. Russell, P. M. Lahti, S. Thayumanavan, *ACS applied materials & interfaces* 2014, *6*, 11376-11384; c) Q. An, F. Zhang, L. Li, J. Wang, J. Zhang, L. Zhou, W. Tang, *ACS applied materials & interfaces* 2014, *6*, 6537-6544; d) L. Beverina, M. Drees, A. Facchetti, M. Salamone, R. Ruffo, G. A. Pagani, *European Journal of Organic Chemistry* 2011, *2011*, 5555-5563; e) G. Chen, H. Sasabe, T. Igarashi, Z. Hong, J. Kido, *Journal of Materials Chemistry A* 2015, *3*, 14517-14534; f) S. Wang, L. Hall, V. V. Diev, R. Haiges, G. Wei, X. Xiao, P. I. Djurovich, S. R. Forrest, M. E. Thompson, *Chemistry of Materials* 2011, *23*, 4789-4798; g) U. Mayerhoffer, K. Deing, K. Gruss, H. Braunschweig, K. Meerholz, F. Wurthner, *Angewandte Chemie* 2009, *48*, 8776-8779.

[3] a) G. Wei, S. Wang, K. Sun, M. E. Thompson, S. R. Forrest, *Advanced Energy Materials* 2011, *1*, 184-187; b) G. Wei, X. Xiao, S. Wang, J. D. Zimmerman, K. Sun, V. V. Diev, M. E. Thompson, S. R. Forrest, *Nano letters* 2011, *11*, 4261-4264; c) G. Chen, H. Sasabe, Z. Wang, X. F. Wang, Z. Hong, Y. Yang, J. Kido, *Advanced materials* 2012, *24*, 2768-2773; d) X. Xiao, G. Wei, S. Wang, J. D. Zimmerman, C. K. Renshaw, M. E. Thompson, S. R. Forrest, *Advanced materials* 2012, *24*, 1956-1960; e) D. Yang, Y. Jiao, L. Yang, Y. Chen, S. Mizoi, Y. Huang, X. Pu, Z. Lu, H. Sasabe, J. Kido, *J. Mater. Chem. A* 2015, *3*, 17704-17712; f) D. B. Yang, L. Yang, Y. Huang, Y. Jiao, T. Igarashi, Y. Chen, Z. Y. Lu, X. M. Pu, H. Sasabe, J. Kido, *ACS applied materials & interfaces* 2015, *7*, 13675-13684; g) L. Yang, D. Yang, Y. Chen, Q. Luo, M. Zhang, Y. Huang, Z. Lu, H. Sasabe, J. Kido, *RSC Adv.* 2016, *6*, 1877-1884; h) D. Yang, H. Sasabe, Y. Jiao, T. Zhuang, Y. Huang, X. Pu, T. Sano, Z. Lu, J. Kido, *Journal of Materials Chemistry A* 2016, *4*, 18931-18941.

[4] a) G. Chen, H. Sasabe, Y. Sasaki, H. Katagiri, X.-F. Wang, T. Sano, Z. Hong, Y. Yang, J. Kido, *Chemistry of Materials* 2014, *26*, 1356-1364; b) L. Yang, Y. Zhu, Y. Jiao, D. Yang, Y. Chen, J. Wu, Z. Lu, S. Zhao, X. Pu, Y. Huang, *Dyes and Pigments* 2017, *145*, 222-232.

[5] D. Yang, H. Sasabe, T. Sano, J. Kido, *ACS Energy Letters* 2017, *2*, 2021-2025.

[6] a) L. Beverina, P. Salice, *European Journal of Organic Chemistry* 2010, *2010*, 1207-1225; b) S. Yagi, H. Nakazumi, *Top Heterocycl Chem* 2008, *14*, 133-181.

[7] a) M. Q. Tian, M. Furuki, I. Iwasa, Y. Sato, L. S. Pu, S. Tatsuura, *Journal of Physical Chemistry B* 2002, *106*, 4370-4376; b) D. Yang, Q. Yang, L. Yang, Q. Luo, Y. Huang, Z. Lu, S. Zhao, *Chemical communications* 2013, *49*, 10465-10467.

[8] H. J. Chen, M. S. Farahat, K. Y. Law, D. G. Whitten, *Journal of the American Chemical Society* 1996, *118*, 2584-2594.

[9] a) Q. Liu, X. M. Xu, W. Q. Sang, *Spectrochim Acta A* 2003, *59*, 471-475; b) V. I. Bystrenina, A. D. Shebaldova, I. V. Lizak, V. A. Sedavkina, M. K. Krasheninnikova, Khimiko-Farmatsevticheskii Zhurnal *Pharmaceutical Chem. J* 1982, *16*, 65-67.

[10] L. Yang, Q. Q. Yang, D. B. Yang, Q. Luo, Y. Q. Zhu, Y. Huang, S. L. Zhao, Z. Y. Lu, *Journal of Materials Chemistry A* 2014, *2*, 18313-18321.

[11] P. W. M. Blom, V. D. Mihailetchi, L. J. A. Koster, D. E. Markov, *Advanced materials* 2007, *19*, 1551-1566.

[12] M. C. Scharber, D. Wuhlbacher, M. Koppe, P. Denk, C. Waldauf, A. J. Heeger, C. L. Brabec, Advanced materials 2006, 18, 789-+.

[13] B. Kan, Q. Zhang, M. Li, X. Wan, W. Ni, G. Long, Y. Wang, X. Yang, H. Feng, Y. Chen, *Journal of the American Chemical Society* 2014, *136*, 15529-15532.

[14] a) M. Li, F. Liu, X. Wan, W. Ni, B. Kan, H. Feng, Q. Zhang, X. Yang, Y. Wang, Y. Zhang, Y. Shen, T. P. Russell, Y. Chen, *Advanced materials* 2015, *27*, 6296-6302; b) B. Walker, A. B. Tomayo, X. D. Dang, P. Zalar, J. H. Seo, A. Garcia, M. Tantiwiwat, T. Q. Nguyen, *Advanced Functional Materials* 2009, *19*, 3063-3069.

[15] C. Luo, Q. Zhou, G. Jiang, L. He, B. Zhang, X. Wang, *New J Chem* 2011, *35*, 1128.

10.1002/chem.201705140

FULL PAPER

Text for Table of Contents

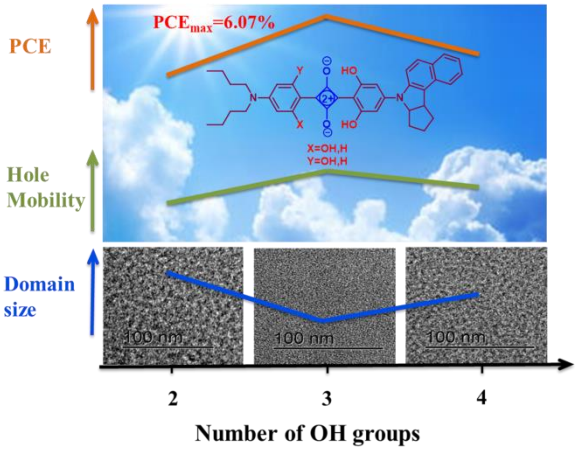

A series of unsymmetrical squaraine derivatives bearing two, three or four hydroxyl (–OH) substituents, namely USQ-2-OH, USQ-3-OH, or USQ-4-OH, were designed and synthesized to investigate the effect of the hydroxyl number on the optoelectronic properties of squaraine derivatives . In contrast to the current findings that "larger number of hydroxy substituents in SQ derivatives may trigger better OPV performance", we found that the trihydroxy substituted USQ-3-OH shows the best photovoltaic performance.

*Jianglin Wu,[a§] Changfeng Si,[b§] Yao Chen,[a] Lin yang,[a] Bin Hu,[a] Guo Chen,[*b] Zhiyun Lu,[a] and Yan Huang[*a]*

1-8

Achieving photovoltaic devices showing high short circuit current approaching 15 mA cm^{-2} through a trihydroxyl substitution strategy on an unsymmetrical squaraine dye